# 3D Geological Modeling using Sketches and Annotations from Geologic Maps

Ronan Amorim* Emilio Vital Brazil† Faramarz Samavati‡ Mario Costa Sousa§
University of Calgary

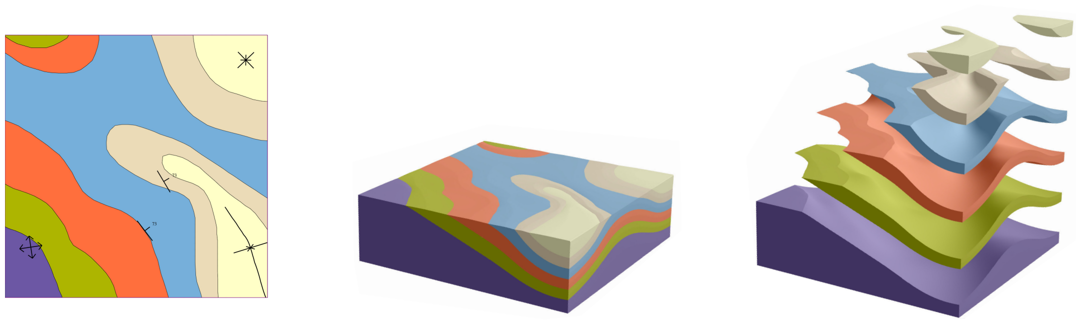

**Figure 1:** *Interpreting a sketched geologic map to generate a 3D geologic model. From left to right, sketched geologic map, generated 3D model, and exploded view of the model.*

## Abstract

Constructing 3D geological models is a fundamental task in oil/gas exploration and production. A critical stage in the existing 3D geological modeling workflow is moving from a geological interpretation (usually 2D) to a 3D geological model. The construction of 3D geological models can be a cumbersome task mainly because of the models' complexity, and inconsistencies between the interpretation and modeling tasks. To narrow the gap between interpretation and modeling tasks, we propose a sketched based approach. Our main goal is to mimic how domain experts interpret geological structures and allow the creation of models directly from the interpretation task, therefore avoiding the drawbacks of a separate modeling stage. Our sketch-based modeler is based on standard annotations of 2D geological maps and on geologists' interpretation sketches. Specific geological rules and constraints are applied and evaluated during the sketch-based modeling process to guarantee the construction of a valid 3D geologic model.

**CR Categories:** I.3.3 [Computer Graphics]: Three-Dimensional Graphics and Realism—Applications

**Keywords:** sketch-based modeling, geology, geologic maps

## 1 Introduction

Geology is the science that studies the Earth. More specifically, structural geology studies the geometry and formation of rock bodies, and the processes, such as folds and faults, that have shaped them. The study of such structures is important for understanding and predicting natural hazards such as earthquakes, and also for the evaluation and exploration of natural resources such as minerals, hydrocarbons (oil/gas), and groundwater.

Oil/gas exploration and production (E&P) involve economically valuable, but complex tasks. They comprise workflows with pipelined processes depending on a multitude of variables, with datasets coming from interrelated disciplines of geophysics, geology, reservoir engineering throughout the E&P life cycle. In this context, 3D geological models play a central role, depicting the fundamental geometry and topology of geological structures and related properties. These models are used as input to subsequent modeling and processes in the E&P cycle, including reservoir flow simulators allowing domain experts to experiment different scenarios, thus enabling better, informative decision-making.

There are several challenges in creating 3D geological models. The first challenge is the need of manual intervention to create such models. The process of creating 3D models of geological structures involves several interpretive steps, mainly because the available data is limited, sparse and multi-scale, and presenting high degrees of uncertainty. Despite advances in computational tools and methods applied to geology, automatic methods are not enough, and tools for an interactive manipulation and creation of 3D geological models are still necessary.

The second challenge is the modeling workflow. In geology, as well as in some engineering fields, the modeling starts with 2D sketches drawn by a geologist (Figure 2) that are later manually translated into a 3D model by a different expert in modeling. The reason these two activities are separated is because moving from interpretation to a full 3D reservoir model ready for simulation is a complex and time consuming task. Moreover, it requires high levels of expertise on each step of the workflow. The whole process is cumbersome due to the lack of computational tools providing a consistent translation from 2D sketches to 3D digital models. In addition, different results are achieved given the interpretive nature of the task – i.e. different interpretations generate different 3D digital models. Even though experts in modeling try their best to construct accurate geologic models from the geologists' interpretations results, the latter often do not recognize their interpretations in the final constructed model. On the other hand, modelers frequently question the lack of consistency of the interpretations they have to rely on [Dulac 2011]. Therefore, inconsistencies between the geologists' interpre-

*e-mail:rmamorim@ucalgary.ca
†e-mail:evbrazil@ucalgary.ca
‡e-mail:samavati@ucalgary.ca
§e-mail:smcosta@ucalgary.ca

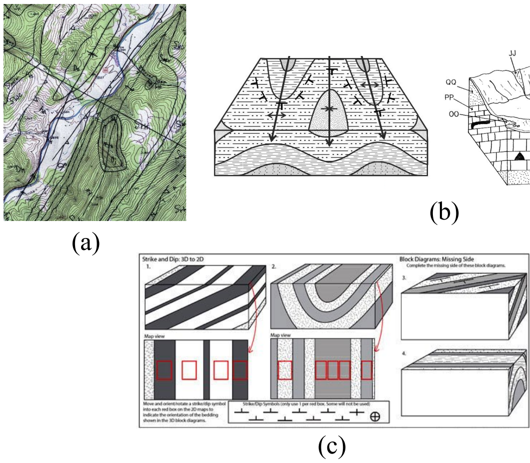

(a) (b) (c)

**Figure 2:** *2: Sketching on geologic maps is used extensively for spatial skills development, structural geology studies, data interpretation, and field exercises. (a) Hand drawn geologic features on usgs 1:24,000-scale topographic map [Donaldson and Hopkins 2003] Source: West Virginia Geological and Economic Survey, Morgantown, WV; (b) (left) Sketches reviewing contacts, strike, dip, and plunge; (right) geologic structure and topography in a sketched block diagram. Source: Dr. Miriam Helen Hill, Physical and Earth Sciences, Jacksonville State University, Jacksonville, AL, 1990 and 2014; (c) Worksheet covering structural geology concepts. Students move and rotate the strike and dip symbols into the red boxes placed on top of geologic maps to indicate the orientation of bedding shown in the block diagrams. For the Block Diagram section, students sketch the missing side of the diagrams by using the information on the other two sides, aiming at improving spatial skills perception [Garnier et al. 2014].*

tation and the 3D shape produced by the modeler leads to a inefficient production cycle.

The third challenge is that geologic models must follow a set of geological rules to be valid. An example of such rules is that horizons (surfaces separating two rock layers) must not self-intersect [Caumon et al. 2009]. Creating models that fail to comply with some of these rules can lead to serious problems specially when they are used for simulations. Moreover, fixing such problems in latter stages of the modeling can be a tedious and difficult task.

The goal of this work is to enable a rapid creation of conceptual 3D geological models based on a sketch-based approach. We propose the modeling of 3D geological structures using a sketch-based modeling metaphor based on standard annotations of 2D geologic maps (see Figure 1). This approach helps mitigate the previously described challenges by first permitting an interactive intervention in the modeling of 3D geological structures. Secondly, closing the gap between interpretation and modeling by providing means of creating a conceptual 3D geological model directly from the interpreters sketch of a geologic map. Finally, in our 3D model construction, some fundamental geological rules are imposed from the beginning by implementing them directly on the geologic map sketch.

Creating 3D objects, in general, in a 3D environment may require hours of work and specialized training. To alleviate this problem, sketch-based modeling (SBM) tries to mimic the natural way people communicate ideas through 2D drawings and translate it into 3D models. However, one of the main challenges in the SBM area of research is how to fill the gap of information of going from 2D to 3D. Geological maps and their symbols and annotations help to reduce the ambiguity of the depth in 3D geological structures. These 2D aerial maps provide a 3D description of rocks, with their structures and contacts, in a region through a rich set of standardized symbols. Despite the current advances in 3D modeling of geological structures, the existing 3D geological modeling approaches do not take advantage of the natural language of the geologists, instead they rely on the windows, icons, menus, pointer (WIMP) paradigm. Such WIMP based tools require specialized training, therefore, making it difficult for geologists to create conceptual 3D geological models to more easily evaluate their interpretation and avoid mistakes.

Our main contribution is an integrated system that mimics the traditional workflow used by geologists. It combines geologic maps and SBM to create 3D geologic models. The system interprets sketches and recognize symbols; and, under geological constraints, generates complex multilayer 3D models. The proposed system also automatically decides the age of the rock layers (which layer is on top of the other) based on the provided symbols and annotations to avoid the tedious task of manually defining their sequence, supporting the idea of rapid prototyping and also avoiding easy-to-make mistakes. Moreover, geological rules are imposed directly on the sketch enabling the creation of valid geologic models.

The rest of this paper is organized as follows. Related work is presented in Section 2. In Section 3 we provide background material in geological concepts and mapping. Section 4 presents an overview of our system. Section 5 explains the method used for recognizing geologic map symbols; in Section 6 we discuss how sketched curves of regions are processed and interpreted. We show how to combine all information to generate 3D models in Section 7. In Section 8 we present and discuss some results obtained using the proposed approach. Finally, in Section 9 we present the conclusions and future work.

## 2 Related Work

The workflow for creating geological models is discussed by Dulac in [Dulac 2011]. He describes the creation of such models as two separate tasks: interpretation and modeling. Modeling depends on the interpretation task and, as Dulac pointed out, interpreters and modelers often disagree on each other's work. Moreover, as discussed by Bond et al. [Bond et al. 2007], interpretation is inherently uncertain and different interpreters may make different interpretations of the same geological structure. Evans [Evans 2003] calls this gap in the modeling process of "Valley of Death" and advocates for a better integration between the interpretation and modeling tasks.

The importance of recent advances on 3D modeling technologies, as well as requirements of geological modeling, are discussed by Turner [Turner 2006]. He describes geo-objects as 3D objects of complex geometry and topology, with scale dependency and hierarchical relationships, and also having heterogeneous properties. Therefore, specific geological modeling systems are required, since conventional modeling systems are designed to construct man-made structures with more regular shapes. Moreover, as presented by Caumon et al. [Caumon et al. 2009], geological structures configurations present specific rules that should be addressed by modeling systems to avoid geologically impossible situations, e.g., self-intersecting surfaces.

Many works have explored SBM as means of providing more natural ways to create 3D models [Igarashi et al. 1999; Cherlin et al. 2005; Nealen et al. 2007; Orbay and Kara 2012]. Olsen et al. [Olsen et al. 2011] combines image-assisted SBM of 3D objects with sketch-annotations. Such annotations are iconic symbols to indicate modeling operations on the object being sketched. Their system is a good example of combining annotations with 3D modeling as proposed in our work. However, in our work we propose to mimic how geologists sketch using geologic maps instead of creating our own sketching language. Our models have different contraints in addition to geologic rules that must be satisfied. Moreover, geologic symbols are composed of different parts that have different effects on the 3D model depending on their positioning, orientation, and size.

SBM has also been previously applied to geological modeling. Amorim et al. [Amorim et al. 2012] present an SBM system for modeling geological horizons. The presented system provides a set of sketch-based operators to help experts in geology to edit, model and augment horizons. However, their system focus mainly in the augmentation of previously extracted (using a semi-automatic method) horizons. To create new horizons from scratch the approach limits to the creation of an initial Coons Surface from 4 strokes on the faces of a seismic cube. This initial surface usually needs a careful and long process of augmentation to get to a final desired shape. Lidal et al. [Lidal et al. 2012] present a comparison between two rapid sketch-based 3D geological modeling tools. The presented tools are based on predefined features such as rivers and ridges/mountains or valleys and are on the interpolation of user drawn curves on cross-sections and top view.

Sketch-based approaches have also been used to create simple illustration of geological scenarios. Natali et al. [Natali et al. 2012] uses a sketch-based approach to create rapid illustration of geology from cross-sections drawing. Since the drawing is completely performed in a single cross section and no other information such as symbols are provided, the generated 3D model is actually 2.5D, representing the extrusion of the cross-section. Lidal et al. [Lidal et al. 2013] present a system to communicate geologists interpretations of seismic/slices (cross-sections) and how they derived their interpretation. The system proposes a flip-over metaphor for sketching individual steps in a story reflecting the steps of the interpreter. However, their work is intended to record the interpretation steps and not to create a 3D geological model.

For a further reading in geological modeling we refer the reader to the work of Natali et al. [Natali et al. 2013], where the authors present a state-of-the-art paper on terrain and geological modeling. They compare types of surface representation and approaches to construct 3D geological models, including sketch-based modeling approaches.

# 3 Background

Geologic maps, despite being represented on a 2D media, are considered the most convenient way to represent and work with the spatial disposition of rocks [Maltman 1990]. These maps are usually made from outcrop information but, since not all rocks are exposed, additional data such as boreholes and soil type can be used to create them [Lisle 2004]. Geologic maps depict geologists interpretations of the areal distribution of different rock bodies and surficial materials [Spencer 1993]. Moreover, through a rich set of symbols, 2D geologic maps are able to convey the 3D configuration and shape of geological structures by indicating, for instance, strikes and inclination of dipping rock layers, faults, and folds (Figure 2). Familiarity with geologic maps is an important aspect of a geologist's training. With practice, a geologist can apply geological principles and constraints being able to picture how rocks are arranged in 3D beneath the surface and how they had been before erosion [Maltman 1990; Bolton 1989]. The following sections describe some geological concepts and structures, what they represent in 3D and how they are depicted in a geologic map.

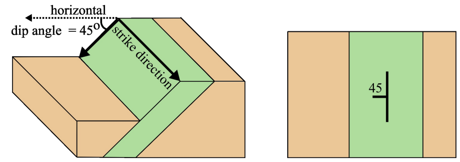


**Figure 3:** *Dip and strike of an inclined rock bed and respective geologic map. In (a), illustration of dip and strike concept. In (b) geologic map containing dip and strike and two different rock layers separated by a geologic contacts line.*

## 3.1 Geologic Contacts

Within a geological formation there are usually distinct rock beds. These beds can be identified based on their color, composition, lithology, etc. Contacts between any two rock beds within a series are called conformable deposition contacts [Davis and Reynolds 1996]. These contacts are represented on geological maps as means of lines indicating their intersection with the ground [Spencer 1993] (Figure 3(b)). This conformable deposition may be interrupted and followed by rock deformations or erosion. When deposition restarts, a different contact is created which is called surface of unconformity. This type of contacts separates two different rock bed series and is represented on maps the same way as conformable deposition contacts, i.e., lines representing its intersection with the ground.

Unconformities can truncate any conformable deposition contacts or older unconformities and can be truncated by newer unconformities [Platt and Challinor 1974]. The ages of the deposits (or rock beds) indicate their order, i.e., newer ones are on top of older ones. Conformable deposition contacts do not truncate each other nor truncate unconformities, therefore, any line on a map that truncates any other line can only represent an unconformity. However, lines that do not truncate any other line can still represent unconformities and are usually indicated as unconformities by other means such as a legend containing all the different rock series.

Since we are modeling rock layers, which are 3D solid objects, there is a set of natural rules that must be followed in order to create a valid representation of the subsurface. We considered, as a proof of concept, the following subset of geologic rules: (1) contacts must not self-intersect; (2) contacts always define closed regions on a map; (3) a rock layer cannot be adjacent to itself; (4) a specific rock layer can exist only in one series.

## 3.2 Dip and Strike

Rock beds and other geological layers and surfaces are said to dip if they are not horizontal. A dipping structure has two components: magnitude and direction. The magnitude is usually given by the maximum angle of inclination of a geological surface from a horizontal plane and it is between $0^\circ$ to $90^\circ$ (see Figure 3(a)). The dip direction is the direction in which such surfaces are inclined and can be visualized as the direction that a drop of water would follow if poured on the surface [Tarbuck et al. 2011; Lisle 2004]. The strike, in turn, is the direction of the line created by the intersection of the inclined surface with a horizontal plane.

2D geologic maps present dip and strike by means of symbols. On a geological map the symbol representing the dip and strike is represented by two lines and a number, the longer line represents the strike direction while the dip direction and the angle are represented by the shorter line and the accompanying number (see Figure 3 (b)). Geologists on the field try to measure as many as possible dip and

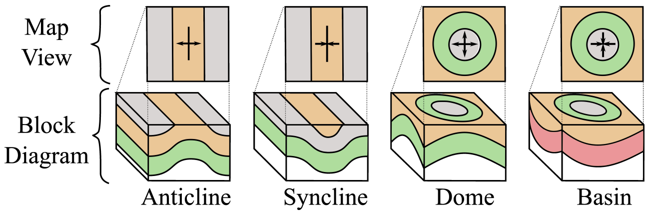


**Figure 4:** *Illustration of geologic folds with their respective map representation and 3D geologic model.*

strike of sedimentary strata. These data, combined with description of rocks on a geologic map or an aerial photograph, can be used to infer the orientation and shape of the rocks [Tarbuck et al. 2011].

### 3.3 Folds

Folds are conspicuous structures that can form in practically any rock type and depth. They result of rock deformation caused by movements that take place within the earth [Maltman 1990; Johnson 1976]. Besides being visually attractive structures, they can also be of great economic importance as oil traps and in the search of mineral resources [Fossen 2010].

Folds are wave-like structures and those which are cylindrical can be classified as anticlines or synclines. Anticlines are upfolds with older rocks in the middle, and synclines are downfolds with younger rocks in the middle. Anticlines and synclines are represented in a geologic map with a symbol that consists of a line, representing where the axial surface intersects the ground, and arrows indicating the direction of younger beds. Different from anticlines and syncline folds, some folds are non-cylindrical, e.g., basins and domes. Domes are classic hydrocarbon traps, and are similar to a cereal bowl turned upside-down [Fossen 2010], i.e., the beds dip uniformly in all directions alway from the center. Basins beds, in turn, dip in all directions towards the center. When eroded, basins and domes create circular patterns on the surface. Domes and basins are represented in a geologic map with a symbol consisted of four arrows, indicating the direction of younger beds.

Figure 4 presents the four types of folds described and their respective geologic map representation and symbols.

### 3.4 Faults

Faults are created by the same forces that create folds. However, rocks can present a different response to such forces by breaking instead of keeping the layers continuous by folding. Faults are fractures in the crust along which appreciable displacement has occurred as result of earth movements [Lisle 2004].

Faults be can categorized in three main groups: dip-slip, strike-slip, and oblique-slip faults. As their names suggest, their categorization depends on the slip direction of the rocks on the fault plane. Dip-slip faults are those whose rocks movements are close to vertical and are caused by compressional or tensional stresses. Strike-slip faults are those where the movement is close to horizontal and are caused by shear stresses. Oblique-slip faults are a combination of dip-slip and strike-slip faults. Figure 5 depicts two types of dip-slip faults and an example of strike slip fault. Two examples of dip-slip faults are the *normal* and *reverse* faults. Normal faults are caused by tensional forces pulling the rock in opposite directions, while reverse faults are caused by compressional forces.

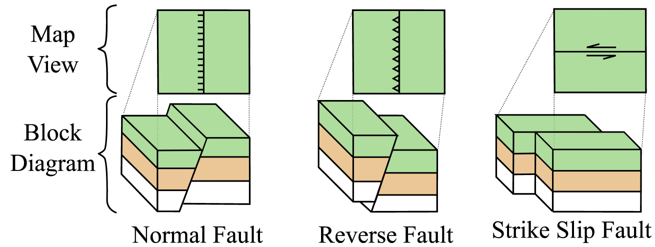


**Figure 5:** *Three different types of faults and their map representation. Normal and reverse faults are examples of dip-slip faults. More specifically normal faults are caused by tensional stresses while reverse faults by compressional stresses. Strike-slip faults are caused by shear stresses.*

## 4 System Overview

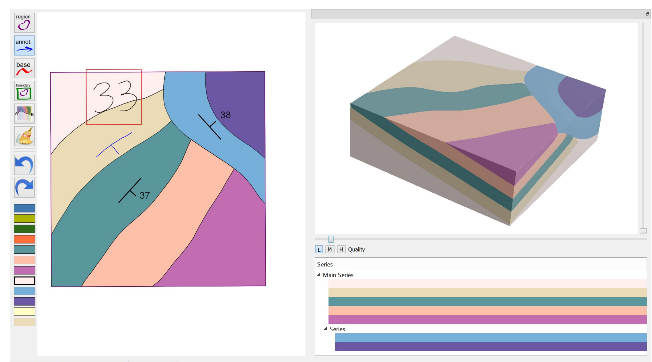

**Figure 6:** *System overview: from hand-drawn symbols and annotations (left) to a 3D geological model (right). A geologic map is sketched on the left, including geologic contacts, symbols, and annotations (handwritten dipping angles). The system checks sketches for compliance with some geological rules and automatically defines the appropriate sequence of the rock layers (bottom right). The 3D geological model (top right) is generated and modified as the user sketches.*

The proposed system translates 2D sketches of contacts and geologic symbols into a 3D model. It starts with a 2D canvas containing a predefined map boundary where geologic symbols and contacts are sketched. To improve the precision when interpreting the sketches, the system has three options of sketching pens: one for sketching contacts and two pens for sketching geologic symbols. By interpreting sketched contacts and symbols, the system automatically recognizes unconformities and the appropriate age (sequence) of rock layers and geological series. These series are then displayed on a tree view structure. As the map is sketched the system checks for compliance with geologic rules then a 3D model is created *on-the-fly* and displayed for visual inspection. In summary the system is composed of a 2D sketching area, a 3D model view, a series tree view, and a toolbar for selecting pens and rock types. In Figure 6 we present the system interface.

Different geologic symbols have different meanings and provide different information that helps defining the 3D arrangement of the rock layers. In the 3D modeling point of view, geologic maps have many symbols with redundant information. In this work, we chose to implement only a subset of geologic symbols, namely, dip-and-strike, anticline, syncline, dome, basin, normal fault and reverse fault. We can divide this subset of symbols into two different groups. The first group contains multistroke symbols that

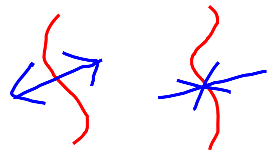

**Figure 7:** *Sketch of geologic symbols using two pens. The fixed part of the symbol is sketched with the blue pen while the varying one (base stroke) is sketched with the red pen.*

are composed only by fixed parts, i.e. dip-and-strike, dome, basin. The second group is composed by multistroke symbols that have one fixed part and a base stroke that can have any shape, i.e. synclines, anticlines, and faults. We designed the system to have two different pens for sketching geologic symbols, one for fixed parts and the other for base strokes. The recognition is triggered based on a time-out from the last stroke of the first pen. Symbols from the first group, which contains only a fixed part, can be sketched using only the first pen. Dip-and-strike and fault symbols also require an extra information, which is the dipping angle. Just after those symbols are drawn, the system will request the handwritting of the angle value.

Sketching contacts is done using a third type of pen. Every sketch defines a new closed region representing a rock layer. Contacts lines can be drawn on different levels of details by zooming in or out, depending on the desired precision. When a new contact is interrupted by an existing contact, the latter becomes an unconformity, which defines a new series. The rock type (color) can be selected prior to sketching a contact or suggested by the system in case it conflicts with a geologic rule. At any moment it can be changed by a drag and drop feature, subject to the same geologic rules. The tree structure is updated providing a visual feedback about the validity of the geologic series. As soon as the model is validated, the system creates a 3D geologic model for inspection.

## 5 Symbol and Hand-Writing Recognition

To mitigate the problem of recognizing a symbol that has a part that varies in shape and length we separate the symbol sketching in two parts. A first pen allows the drawing of the varying part of the symbol, and a second pen the fixed part. For the symbols considered in this work, the varying part is always a single curve of any shape and length. The fixed part however, can be composed of multi-strokes. We developed a multi-stroke symbol recognizer for the fixed part that uses three features as discriminants and that are matched against symbol templates. Figure 7 presents examples of geologic symbols that are recognized with the varying part in red, which we call base stroke, and the fixed part in blue. The question in multi-stroke symbol recognition is how to combine multiple strokes into a single symbol. The same symbol can be drawn in a variety of ways depending on the order and direction of strokes. Some approaches simplify the problem by requiring the strokes to be drawn on a specific order [Donmez and Singh 2012]. Others, solve this problem using a combinatorial approach [Anthony and Wobbrock 2010; Anthony and Wobbrock 2012]. Image-based recognizers, on the other-hand, do not store any direction information, and do not suffer the problems with multi-stroke symbols [Kara and Stahovich 2005; Hse and Newton 2004]. However, the orientation of some symbols are also an important information to be extracted from geologic symbols.

Our symbol recognizer is based on the approach proposed by Glucksmann [Glucksman 1967]. In our approach each stroke is defined by a line containing a sequence of 2D points. From these points we compute one axis of maximum variance of all strokes' points using Principal Component Analysis (PCA). We rewrite the coordinates of the points using the PCA center and axes, making it translation and rotation invariant. Then we normalize them to the unit square to make the symbol scale invariant. We use the PCA angle information as part of the 3D model computation and to draw the template symbol on the 2D canvas. After this, we discretize the $x$ axis (principal component) into 64 bins. For each bin $b$ we compute the number of intersections of the symbol strokes with the bin vertical line $l_b$, where $l_b = (\frac{2b+1}{128} - 0.5, y)$. However, since we are also interested in getting a good approximation of the intended angle that a symbol was drawn, the PCA alone can lead to problems for symmetric symbols. Imagine the case of two dip-and-strike symbols where the first points up, while the second points down. The vector $(1, 0)$ and $(0, 1)$ are perfect principal components for both symbols. If we use these vectors to compute the angle of the symbols both would yield $0°$, but we know the second is $180°$. To solve this problem we need to orient both vectors consistently. To accomplish this we compute the density of points on left and right quadrants and orient the first vector to point in the direction of greater density. We do the same for the second vector, but based on the top and bottom quadrants.

Two more features are important to distinguish symbols. First, the width and height aspect ratio. Second, the intersection with the base stroke, which includes the distance between intersection points as well as the number of intersections. In order to combine the three features we use the following formula:

$$D_t = \underbrace{w_v \|\vec{v_t} - \vec{v}\|^2}_{\text{vertical intersections}} + \underbrace{w_r |r_t - r|^2}_{\text{width/height ratio}} + \underbrace{w_i (\|\vec{i_t} - \vec{i}\|^2 + |n_t - n| P_n)}_{\text{intersections}}, \tag{1}$$

where the subscripts $t$ represent the feature of the template symbol (predefined symbol we want to match), $v$ represents the vertical intersections vector, $r$ the width to height ratio, $i$ the intersection point, $n$ the number of intersections, $P_n$ is a penalty for having a different number of intersections from the template symbol, and $w_v$, $w_r$, and $w_i$ are weights. For the symbols we need to recognize we found experimentally that a good choice of parameters is: $w_v = 0.273$, $w_r = 0.273$, $w_i = 0.454$, $n_p = 3.0$. The recognition threshold is also experimentally set to 21, which means that if for all $t$ $D_t > 21$ the sketched symbol will not be recognized.

Finally, to recognize handwritten angles for the dip-and-strike and fault symbols, we rely on the Tesseract OCR engine [Tesseract OCR 2014] trained with samples of handwritten digits.

## 6 Contacts Graph

In this work we developed a graph-based representation to capture the sketched geologic contacts. This graph is used to calculate unconformities, which series a rock layer belongs, rock-layer adjacencies, and to check compliance with geologic rules (Section 3.1). One alternative to this graph-based approach would be a rasterization of the sketches [Olsen et al. 2011]. Nonetheless, rasterization would pose a problem for sketching contacts with different levels of detail since we would need very high resolutions for one single fine detail.

When a contact curve is sketched it is first super-sampled by equidistant points based on the zoom factor, to take into account the level of details. Then a reverse Chaikin filter is applied four times to remove noise from the input. If the new curve is valid after the filtering, it is used to update the contact graph. According to geologic rules a curve is invalid if it is outside the map, has self-intersections, or has only one intersection with the graph. Every new valid curve generates a closed region that represents a visible part of a rock layer, and for now on, we say this curve belongs to this rock layer. There are two possibilities of updating the graph depending on the number of intersections with the curve. If there is no intersection, the curve is converted into a new connected component of the contacts graph. If there are 2 or more intersections the segment between the two first intersections is added to the connected component of the graph intersected. Each vertex of our graph representation contains information of its 2D position on the map, a list of neighboring rock layers, and *id* (reference to the rock layer the vertex belongs). Using the vertices' *ids* and list of neighbors we can check the geologic rule that forbids a rock layer to be adjacent to itself.

To decide if a closed region is an unconformity we look for *T* junctions vertices and check their adjacent vertices *ids*. Based on these unconformities we build a *series tree* composed of unconformities and rock layers. This tree represents the hierarchy of unconformities (older on top) and all leaves are rock layers. Using this tree we can decide to which series a rock layer belongs. Therefore, we can check the geologic rule that forbids a rock layer to exist in two different series. Figure 8 illustrates an example of a contacts graph and its corresponding series tree.

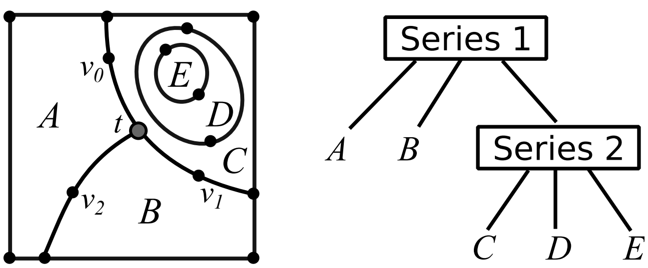


**Figure 8:** *Illustration of contacts graph and corresponding* series tree. *Vertex* $t$ *has* $id = B$ *and neighbors A and C. Vertex* $v_0$ *has* $id = C$ *and neighbor A;* $v_1$ *has* $id = C$ *and neighbor B;* $v_2$ *has* $id = B$ *and neighbor A. Checking the T junction* $t$ *adjacency, the contact containing* $v_0$ *and* $v_1$ *is defined as an unconformity since their ids are equal.*

## 7 3D Geologic Model Creation

Our final 3D geologic model is composed by a combination of implicit surfaces. These surfaces represent the interface between two rock layers defining solid objects. The final solid objects are constructed by Constructive Solid Geometry (CSG) based on the age of rock layers.

Each surface is represented by an iso-value of a function $F : \mathbb{R}^3 \to \mathbb{R}$, that interpolates geologic contacts and dip direction defined by geologic symbols. A geologic series is represented by a single function $F$ and, within this series, contacts are represented by different iso-values. These iso-values are chosen based on the rock layers age, ranging from $0$ (surface on top of the oldest rock layer) to $n$ (surface on top of the $n^{th}$ rock layer). In order to automatically find the sequence of rock layers, we extract their adjacency from the contacts graph. However, only from this adjacency it is not possible to decide whether this sequence is on the proper age order or reversed. To resolve this ambiguity we find whether a point $p$ inside a region within the series is on a syncline or an anticline. We check this by interpolating an implicit surface using the information of the contacts defining this region, and the geologic symbols of the series it belongs. Since we do not have yet the rock layer order information, we arbitrarily interpolate the contacts at this time using zero as its iso-value. Therefore, if $F(p) < 0$, it is an anticline, otherwise it is a syncline. In this work we chose the Hermite-Birkhoff Radial Basis Function (HBRBF) interpolation [Pereira et al. 2011] as our function $F$. HBRBFs create implicit surfaces that can interpolate: values, gradients, or values and gradients at a point in space, which is a good fit for our problem of interpolating contacts and dip directions.

Faults are defined by lines, that represent where they cut the surface, and a dipping angle. Each fault is represented by its own HBRBF, which interpolates the fault line and the dipping angle by including samples with value and gradient. We can define if a point is on left or right of the fault by evaluating this HBRBF function. Based on the type of fault, we create a displacement field for points on the left and another for points on the right.

To create the 3D solid model of each layer, we use the automatically computed hierarchy of rock layers and unconformities and the HBRBF defining each contact. Each rock layer defines a 3D volume that will be combined with the others by CSG boolean operations. To create a rock layer $i$ we subtract the implicit surface with iso-value $i$ by the one with iso-value $i - 1$. Unconformities are created using the series tree, where we subtract each entire series from its parent. Finally, we use the marching tetrahedra method [Treece et al. 1999] to extract the iso-surface of each rock layer.

## 8 Results and Discussion

In this section we present and discuss results obtained using the sketch-based approach proposed in this work. Our approach mimics the traditional workflow used by geologists permitting the creation of 3D geologic models from sketches of geologic maps. The system was implemented for the Microsoft® Surface Pro pen-enabled tablet (Intel® Core™i5-3317U CPU with 1.7GHz, 4GB RAM memory, and Intel® HD Graphics 4000 graphics card). For all created models, the system enables the visual inspection of the 3D geologic models in interactive time. To create the 3D models of this section, using a marching tetrahedra sampling of $50 \times 50 \times 18$, the system took from $0.4$s to $2.8$s depending on the complexity (number of layers, unconformities and faults) of the model. However, to generate the figures in this section in high quality we used a sampling of $200 \times 200 \times 72$, which took from $24$s to $158$s. To facilitate the inspection of the interior of the 3D model we implemented a tool to cut the model, by sketching a line on the map (see Figure 14 (c) and (d)).

Our first results demonstrate that our system is able to reproduce the basic geologic structures described in Section 3, by sketching the corresponding geologic map. In Figure 9 we replicate the four types of geologic folds discussed in Section 3.3. Figure 10 demonstrates the dip and strike symbol (see Section 3.1) and normal and reverse faults discussed in Section 3.4.

In Figure 11 we present the sketching of a geologic map containing an unconformity and the automatically computed hierarchy of geological series and rock layers. In the first step, the sketched map contains two different rock layers within the same geological series. Since there is no geologic symbol (orientation information), the age of the rock layers is ambiguous, and we cannot generate a 3D geological model. In the second step a new contact is included that intersects with an existing one. The region contained by the intersected contact then becomes an unconformity and a new younger geologic series is created. The respective geologic series and their rock layers are displayed hierarchically from older(top) to younger(bottom). In the final step other rock layers are added on both series and dipping information is provided. Based on the

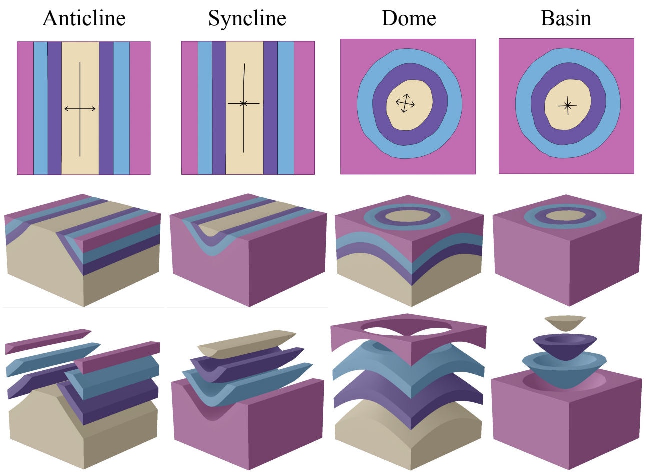


**Figure 9:** *Sketching basic fold structures using specific geologic symbols. First row presents the sketched geologic map. Second row presents the 3D geologic model generated, and third row the same model in an exploded view.*

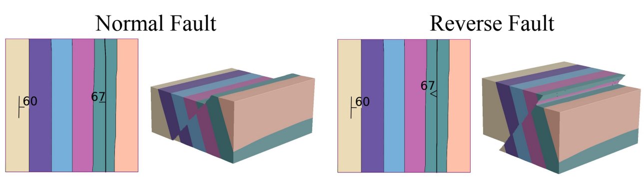


**Figure 10:** *Sketch and 3D geologic model generated for normal and reverse faults. The dip and strike symbol is also sketched to specify the dipping direction of rock beds.*

sketched geologic map the final 3D geologic model is created composed of two geologic series and, as expected, the younger geologic series interrupts the older one.

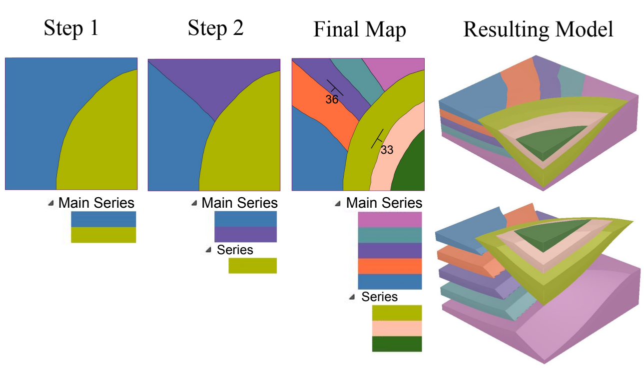


**Figure 11:** *Unconformity and geologic series. In the first step the sketched map contains a single contact that separates two rock layers. In the second step a new contact is created that intersects the existing one defining a new unconformity creating a new geologic series. The final map contains the two geologic series with different rock layers with orientation defined by dip-and-strike symbols.*

A Plunging fold is another interesting structure observed in geologic maps.Such folds leave a $V$ pattern (or $W$ for two consecutive folds) when cutting the ground and the same can be observed on geologic maps. In Figure 12 we model a plunging anticline and a plunging anticline of two folds each. We do so by sketching the $W$ pattern and a single dipping symbol oriented according to the type of fold. In Figure 13 we create a $V$ type plunging anticline using the anticline symbol this time.

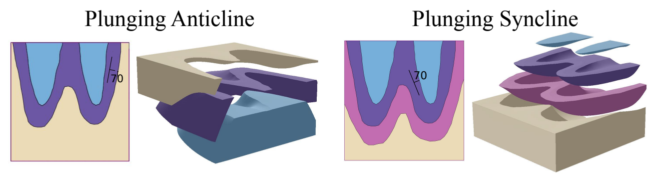


**Figure 12:** *Sketching plunging anticline and syncline folds using a dip-and-strike symbol and* W*-shaped contacts.*

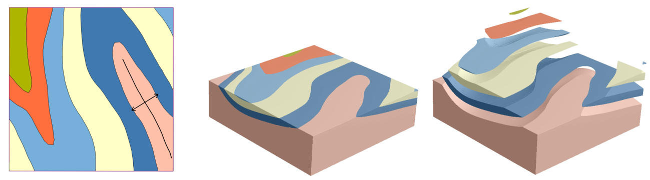

**Figure 13:** *Sketching plunging anticline using anticline symbol and* V*-shaped contacts.*

Finally, in Figure 14 we create a complex model combining more rock layers and symbols. In Figure 14(a) the sketched map contains two geologic series and six dip-and-strike symbols. The 3D geologic model generated is displayed as a block model and as an exploded view with $z$ axis exaggerated. In Figure 14(b) a reverse fault is sketched and in (c) we sketch a cutting line and the interior of the model is inspected. Finally, in Figure 14(d) another fault is sketched and the final 3D geological model is presented using the same cut as before.

As demonstrated in this section, our system is able to reproduce the basic geologic structures and more complex geologic models based on the sketch of the corresponding geologic maps. The system also ensures the compliance with the geologic rules discussed in this paper, creating a valid geologic map that is reflected in a 3D geologic model. Moreover, the 3D model generated respects the constraints provided by the sketched geologic map. Although we can create a great variety of geologic models, the system has some limitations. One example of such limitations is the strike-slip fault structure. This type of fault symbol creates discontinuities on the geologic map and interferes with the proposed contacts graph. Another limitation is recognizing some more complex geologic symbols such as the plunging anticline/syncline. Such symbol is composed of an extra arrow shaped symbol on an end of the symbol axial surface stroke. Finally, when creating the 3D model we assume that all rock layers have the same thickness (by using fixed spaced iso-values). Nonetheless, such thickness could be user-defined or an automatically evaluated from the contacts distances on the map.

## 9 Conclusions and Future Work

In this work we presented a system that enables the geologist to sketch a geological map and obtain a 3D model. It allows the sketching of geological contacts (interfaces between different rock layers), symbols and annotations. Contacts are checked and combined defining different regions on the map. Geologic symbols are recognized from the sketches and assigned to the proper regions within the map. Based on the contacts adjacency and the symbols provided, the system automatically defines which rock layer lies on top of the other. Following the constraints defined on the geologic

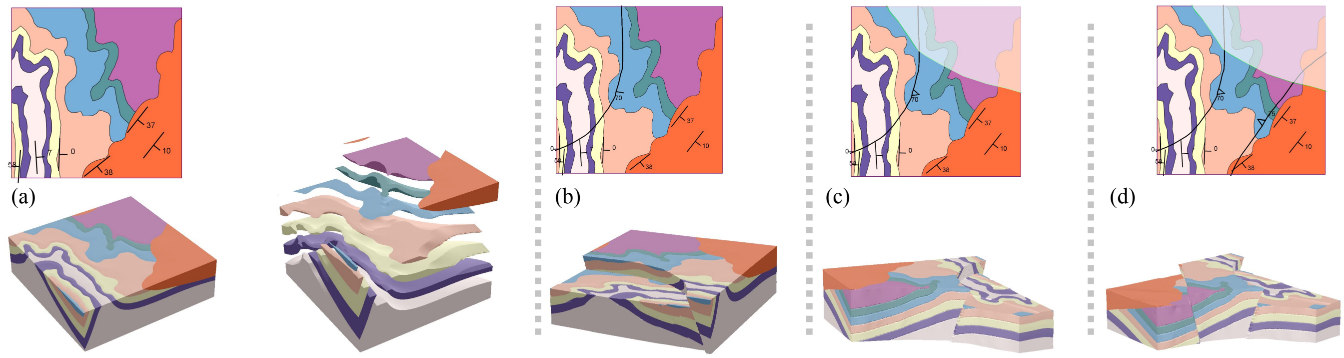


**Figure 14:** *Combining more complex geologic contacts with symbols and unconformity. In (a) the geologic map contains two different geologic series. A fault is sketched and presented in (b). In (c) the interior of the same model is inspected by sketching a cutting curve. A new fault is sketched in (d) and a final 3D geologic model is presented using the previous cut.*

map sketch and the computed sequence of rock layers, a 3D geological model is constructed *on-the-fly*.

To achieve the goal of creating 3D geological models from geologic maps we first recognize the geological symbols in the sketch. For this purpose, we implemented a multi-stroke symbol recognition that enables the system to understand the input sketch. The system also handles input sketches of geologic contacts on a map by creating a graph with such contacts and checking for their validity. Based on the graph constructed, a hierarchy of the rock layers is created and with the help of geologic symbols information, their proper succession is defined. The same information of interfaces and symbols is translated into proper constraints to create the 3D model. To create a 3D geologic model from the 2D map we use a HBRBF interpolation. The final 3D model is then constructed based on the automatic analysis of the sketch (defining the proper succession of rock layers) to create a constructive solid geometry (CSG) tree to combine all HBRBF surfaces.

As future work we plan to approach the limitations discussed in Section 8. For instance, we can enhance the contacts graph representation to handle strike-slip faults. We also plan to include the terrain elevation as a base for the geologic map sketch. Moreover, although not usually present in geologic maps, another possible future work is to enable the configuration of some parameters on structures created by geologic symbols. For instance, fault-slip magnitude, anticline, syncline, dome and basin fold shapes and magnitudes. Finally, more geologic symbols can be included, such as monoclines, plunging and asymmetric anticline and syncline.

## Acknowledgements

We would like to thank our colleagues for their useful discussions and advice, in particular to Joaquim Jorge, TU-Lisbon. Many thanks to Miriam Helen Hill (Jacksonville State University), Bridget Garnier (Carleton College), Ronald McDowell (West Virginia Geological and Economic Survey), and Eric Hopkins (West Virginia University) for providing the illustrations showing the use of hand-drawn sketches and annotations over geological maps. We also thank the anonymous reviewers for their careful and valuable comments and suggestions. This research was supported in part by the NSERC/Alberta Innovates Technology Futures (AITF)/Foundation CMG Industrial Research Chair Program in Scalable Reservoir Visualization and by grants from NSERC (Discovery Grants Program) and GRAND NCE.

## References

AMORIM, R., BRAZIL, E. V., PATEL, D., AND SOUSA, M. C. 2012. Sketch modeling of seismic horizons from uncertainty. In *Proceedings of the International Symposium on Sketch-Based Interfaces and Modeling*, Eurographics Association, Aire-la-Ville, Switzerland, Switzerland, SBIM '12, 1–10.

ANTHONY, L., AND WOBBROCK, J. O. 2010. A lightweight multistroke recognizer for user interface prototypes. In *Proceedings of Graphics Interface 2010*, Canadian Information Processing Society, GI '10, 245–252.

ANTHONY, L., AND WOBBROCK, J. O. 2012. $n-protractor: a fast and accurate multistroke recognizer. In *Proceedings of the 2012 Graphics Interace Conference*, Canadian Information Processing Society, GI '12, 117–120.

BOLTON, T. 1989. *Geological Maps: Their Solution and Interpretation*. Cambridge University Press.

BOND, C. E., GIBBS, A. D., SHIPTON, Z. K., AND JONES, S. 2007. What do you think this is? "conceptual uncertainty" in geoscience interpretation. *GSA Today 17*, 4–10.

CAUMON, G., COLLON-DROUAILLET, P., VISEUR, S., AND SAUSSE, J. 2009. Surface-based 3d modeling of geological structures. *Mathematical Geosciences 41*, 927–945.

CHERLIN, J. J., SAMAVATI, F., SOUSA, M. C., AND JORGE, J. A. 2005. Sketch-based modeling with few strokes. In *Proceedings of the 21st spring conference on Computer graphics*, ACM, New York, NY, USA, SCCG '05, The Eurographics Association, 137–145.

DAVIS, G. H., AND REYNOLDS, S. J. 1996. *Structural Geology of Rocks and Regions*, third ed. John Wiley & Sons.

DONALDSON, K., AND HOPKINS, E. 2003. Digital conversion of geologic maps pendleton county, west virginia. Tech. rep., West Virginia University, Department of Geology and Geography, September.

DONMEZ, N., AND SINGH, K. 2012. Concepture: a regular language based framework for recognizing gestures with varying and repetitive patterns. In *Proceedings of the International Symposium on Sketch-Based Interfaces and Modeling*, Eurographics Association, SBIM '12, 29–37.

DULAC, J.-C. 2011. Technology enhances 3-d modeling. *The American Oil & Gas Reporter* (july).

EVANS, S. 2003. The last integration frontier. *E&P February*.

FOSSEN, H. 2010. *Structural Geology*. Cambridge University Press.

GARNIER, B., ORMAND, C., CHANG, M., TIKOFF, B., SHIPLEY, T., AND FORBUS, K., 2014. Using cogsketch to increase sketching and spatial skill development in geoscience classrooms. The Spatial Intelligence and Learning Center (SILC) Showcase January 2014, National Science Foundation Science of Learning Center.

GLUCKSMAN, H. A. 1967. Classification of mixed-font alphabetics by characteristic loci. In *1967 Digest of 1st Annual IEEE Computer Conference*, IEEE.

HSE, H., AND NEWTON, A. R. 2004. Sketched symbol recognition using zernike moments. In *International Conference on Pattern Recognition*, 367–370.

IGARASHI, T., MATSUOKA, S., AND TANAKA, H. 1999. Teddy: a sketching interface for 3d freeform design. In *Proc. of SIGGRAPH '99*, ACM, 409–416.

JOHNSON, W. E. 1976. *Simple Geological Mapwork*. Edward Arnold Publishers Limited.

KARA, L. B., AND STAHOVICH, T. F. 2005. An image-based, trainable symbol recognizer for hand-drawn sketches. *Comput. Graph. 29*, 4 (Aug.), 501–517.

LIDAL, E. M., HAUSER, H., AND VIOLA, I. 2012. Geological storytelling: graphically exploring and communicating geological sketches. In *Proceedings of the International Symposium on Sketch-Based Interfaces and Modeling*, Eurographics Association, Aire-la-Ville, Switzerland, Switzerland, SBIM '12, 11–20.

LIDAL, E., PATEL, D., BENDIKSEN, M., LANGELAND, T., AND VIOLA, I. 2013. Rapid sketch-based 3d modeling of geology. In *Workshop on Visualisation in Environmental Sciences (EnvirVis)*, The Eurographics Association, 31–35.

LISLE, R. J. 2004. *Geological Structures and Maps: A Practical Guide*. Elsevier Butterworth-Heinemann.

MALTMAN, A. 1990. *Geological Maps: An Introduction*. Open University Press.

NATALI, M., VIOLA, I., AND PATEL, D. 2012. Rapid visualization of geological concepts. In *Graphics, Patterns and Images (SIBGRAPI), 2012 25th SIBGRAPI Conference on*, IEEE, 150–157.

NATALI, M., LIDAL, E. M., PARULEK, J., VIOLA, I., AND PATEL, D. 2013. Modeling terrains and subsurface geology. In *Eurographics 2013-State of the Art Reports*, 155–173.

NEALEN, A., IGARASHI, T., SORKINE, O., AND ALEXA, M. 2007. Fibermesh: designing freeform surfaces with 3d curves. *ACM Trans. Graph. 26*, 3, 41–50.

OLSEN, L., SAMAVATI, F., AND JORGE, J. 2011. Naturasketch: Modeling from images and natural sketches. *Computer Graphics and Applications, IEEE 31*, 6 (nov.-dec.), 24 –34.

ORBAY, G., AND KARA, L. B. 2012. Sketch-based surface design using malleable curve networks. *Computers & Graphics*, 0, –.

PEREIRA, T., BRAZIL, E. V., MACŁDO, I., SOUSA, M. C., DE FIGUEIREDO, L. H., AND VELHO, L. 2011. Sketch-based warping of RGBN images. *Graphical Models 73*, 4, 97 – 110.

PLATT, J. I., AND CHALLINOR, J. 1974. *Simple Geological Structures*. Thomas Murby & Co.

SPENCER, E. 1993. *Geologic Maps: A Practical Guide to The Interpretation and Preparation of Geologic Maps*. MacMillan Publishing Company.

TARBUCK, E., LUTGENS, F., AND TASA, D. 2011. *Earth: An Introduction to Physical Geology*. Pearson Prentice Hall.

TESSERACT OCR, 2014. `http://code.google.com/p/tesseract-ocr/`. [Online; accessed 21-April-2014].

TREECE, G. M., PRAGER, R. W., AND GEE, A. H. 1999. Regularised marching tetrahedra: improved iso-surface extraction. *Computers & Graphics 23*, 4, 583–598.

TURNER, A. 2006. Challenges and trends for geological modelling and visualisation. *Bulletin of Engineering Geology and the Environment 65*, 109–127.